



Using Strong Gravitational Lensing to Identify Fossil Group Progenitors

Lucas E. Johnson¹, Jimmy A. Irwin^{1,2} , Raymond E. White, III¹, Ka-Wah Wong^{3,4} , W. Peter Maksym⁵ , Renato A. Dupke^{4,6,7},
Eric D. Miller⁸, and Eleazar R. Carrasco⁹

¹ Department of Physics & Astronomy, University of Alabama, Box 870324, Tuscaloosa, AL 35487, USA; lejohnson4@crimson.ua.edu

² Department of Physics & Astronomy, Seoul National University, Seoul 08826, Republic of Korea

³ Department of Physics & Astronomy, Minnesota State University, Mankato, MN 56001, USA

⁴ Eureka Scientific Inc., 2452 Delmer St., Suite 100, Oakland, CA 94602, USA

⁵ The Harvard-Smithsonian Center for Astrophysics, 60 Garden St., MS-67, Cambridge, MA 02138, USA

⁶ Department of Physics & Astronomy, University of Michigan, 450 Church St., Ann Arbor, MI 48109, USA

⁷ Observatório Nacional, Rua Gal. José Cristino 77, São Cristóvão, CEP20921-400 Rio de Janeiro RJ, Brazil

⁸ Kavli Institute for Astrophysics & Space Research, Massachusetts Institute of Technology, 77 Massachusetts Ave., Cambridge, MA 02139, USA

⁹ Gemini Observatory/AURA, Southern Operations Center, AURA, Casilla 603, La Serena, Chile

Received 2017 October 30; revised 2018 February 7; accepted 2018 March 3; published 2018 April 2

Abstract

Fossil galaxy systems are classically thought to be the end result of galaxy group/cluster evolution, as galaxies experiencing dynamical friction sink to the center of the group potential and merge into a single, giant elliptical that dominates the rest of the members in both mass and luminosity. Most fossil systems discovered lie within $z < 0.2$, which leads to the question, what were these systems' progenitors? Such progenitors are expected to have imminent or ongoing major merging near the brightest group galaxy that, when concluded, will meet the fossil criteria within the look forward time. Since strong gravitational lensing preferentially selects groups merging along the line of sight, or systems with a high mass concentration like fossil systems, we searched the CASSOWARY survey of strong-lensing events with the goal of determining whether lensing systems have any predisposition to being fossil systems or progenitors. We find that $\sim 13\%$ of lensing groups are identified as traditional fossils while only $\sim 3\%$ of nonlensing control groups are. We also find that $\sim 23\%$ of lensing systems are traditional fossil progenitors compared to $\sim 17\%$ for the control sample. Our findings show that strong-lensing systems are more likely to be fossil/pre-fossil systems than comparable nonlensing systems. Cumulative galaxy luminosity functions of the lensing and nonlensing groups also indicate a possible, fundamental difference between strong-lensing and nonlensing systems' galaxy populations, with lensing systems housing a greater number of bright galaxies even in the outskirts of groups.

Key words: galaxies: evolution – galaxies: groups: general – galaxies: luminosity function, mass function – gravitational lensing: strong

1. Introduction

Fossil systems are classically thought to be representative of old, undisturbed galaxy systems where almost all L^* members have been cannibalized by the dominant central elliptical, as dynamical friction draws the massive L^* member galaxies to the center over long timescales. As the central elliptical cannibalizes more galaxies, the magnitude gap between the central elliptical and the next most massive member widens, and mass becomes more concentrated at the center until a “fossil system” is created (Jones et al. 2003). One study of the mass concentration of fossil groups using N -body simulations show some support for this assumption toward fossil system formation (Khosroshahi et al. 2007). Due to the apparent evolved nature of fossil systems and high concentration parameters (Wechsler et al. 2002), it is possible that studying fossil systems can help us understand properties of the early universe and brightest cluster/group galaxy formation. However, exactly how common fossil systems are in the universe is not well constrained.

Jones et al. (2003) originally defined a fossil system to be a galaxy group or cluster with a massive brightest group or cluster galaxy (BGG or BCG) that dominates (by more than two magnitudes in the r band) the rest of the galaxies within $0.5R_{200}$, defined as half of the virial radius of the system, and shows a bolometric X-ray luminosity $L_{X,\text{bol}} \geq 10^{42} h_{50}^{-1} \text{ erg s}^{-1}$. This definition has done well in identifying massive fossil

systems but has the potential to miss poorer fossil groups, along with being less robust for these poor fossil groups (Dariush et al. 2010), since the infall of a lone luminous galaxy would destroy the system's fossil status. To address this, Dariush et al. (2010) proposed altering the classic Jones optical criteria: instead of using $\Delta m_{12} \geq 2.0$, where Δm_{12} is the r -band magnitude gap between the first- and second-rank galaxies, Dariush et al. (2010) require $\Delta m_{14} \geq 2.5$, where Δm_{14} is the r -band magnitude gap between the first- and fourth-rank galaxies. This change would allow for the infall of one or two luminous galaxies without destroying the fossil status of the poorer group. Jones et al. (2003) found that fossil systems should compose between 8% and 20% of all galaxy groups. However, this study was only done for nearby groups and clusters of $z < 0.25$. A more recent study by Gozaliasl et al. (2014) shows that the fossil group fraction for massive galaxy groups ($M_{200} \sim 10^{13.5} M_{\odot}$, where M_{200} is the mass within a sphere of density equal to 200 times the critical density of the universe) is $22\% \pm 6\%$ for $z \leq 0.6$ and $13\% \pm 7\%$ for $0.6 < z < 1.2$ if a $\Delta m_{12} \geq 1.7$ is required.

Since most fossil systems found to date lie within $z < 0.2$, fossil galaxy groups could be old, undisturbed systems, as the infall of any bright galaxy has the potential to destroy their fossil statuses. The Millennium Simulation supports this idea, as it shows fossils being formed near $z = 0.9$ and subsequently being destroyed owing to the infall of a bright L^* galaxy that

breaks the r -band magnitude gap requirement before $z = 0$ (von Benda-Beckmann et al. 2008). However, as some fossils are destroyed in the simulation, others are created as bright members are consumed by the BGG (Ponman et al. 1994), thus establishing the required r -band magnitude gap. This result from the simulation suggests that fossil systems could be more of a “fossil phase” that all groups have a likelihood of passing through as opposed to a unique class of object all their own. There also exists controversial evidence that fossils have a higher-than-expected mass concentration parameter (Khosroshahi et al. 2004, 2006; Sun et al. 2004), although some observations of nearby fossils dispute this (Sun et al. 2009). These pieces of evidence point to fossil systems possibly having different initial conditions than most groups. To further complicate the matter, there are many supposedly old, evolved nearby fossil systems that do not possess cool cores as would be expected from relaxed systems (Khosroshahi et al. 2004, 2006; Sun et al. 2004). These fossil systems needed an energetic event of some kind (such as an active galactic nucleus [AGN] turning on, a burst of star formation, or a group merger) in their recent past to heat up their intragalactic medium (IGM) or destroy any preexisting cool cores, which is at odds with these fossils being relaxed. However, Trevisan et al. (2017) found that star formation histories of nearby fossil BGGs suggested that they grew over time via dry mergers, decreasing the likelihood that star formation alone could combat IGM cooling in the supposedly dense cores of fossils.

Despite the certain existence of fossil progenitors, little observational work has gone into locating any. A progenitor to today’s fossil systems would be a system at a higher redshift with ongoing or imminent major merging, in midassembly of the eventual fossil system’s massive BGG.¹⁰ The amount of merging concluded by $z = 0$ would be sufficient to push the final BGG r -band magnitude 2 mag brighter than any other remaining galaxy member within $0.5R_{200}$. The progenitor could also be more centrally mass concentrated than other nonfossil groups at similar redshifts if fossil systems are a unique set of galaxy groups as some suggest. We expect fossil progenitors to be distinctly different from compact groups, since compact groups do not show velocity dispersions indicative of a deep cluster-like potential well, and the formation of fossil systems is not explained by the merger of galaxies in compact groups (La Barbera et al. 2010). Additionally, N -body simulations from $0 < z < 0.5$ show that a minority of compact groups become fossils given that the mean merger timescales of ~ 10 Gyr for these systems are too great to achieve a $\Delta m_{12} \geq 2.0$ by $z = 0$ (Farhang et al. 2017).

An overarching question in the study of fossil systems is what these groups looked like in the early universe. Are they all old, evolved systems, the inevitable end for all clusters, or are fossils simply a phase that all groups have a probability of transitioning through? While the former explanation is possible, the likelihood that the entire fossil population is composed of isolated, undisturbed groups seems low based on the frequency of mergers in the early universe as seen in simulations. Studies of the Millennium Simulation also cast doubt on this being the sole explanation. Many fossil systems in the simulation form between $0.3 < z < 0.6$, and the fossil

system BGGs were always larger than their nonfossil counterparts (Kanagusuku et al. 2016), suggesting that fossil systems could begin with different initial conditions than most galaxy systems. By studying the Cheshire Cat fossil progenitor system, it has been demonstrated that if two groups merge, the final product has the potential to be a fossil group once the BGGs of the respective groups merge (Irwin et al. 2015). It was estimated that the first- and second-rank galaxies in the Cheshire Cat gravitational lens will merge in 0.9 Gyr, and once this merger concludes, the group will become a fossil system. Further, optical and X-ray observations revealed that the system is composed of two separate galaxy groups undergoing a line-of-sight merger, opening another avenue for fossil system formation: (fossil) group mergers. This second possible formation mechanism offers an explanation for observed non-cool-core fossil systems (as X-ray cooling timescales are typically longer than galaxy merger timescales).

It is known that fossil systems house massive BGGs at their centers (Jones et al. 2003), implying a higher-than-average mass concentration when compared to normal groups of similar richness. This enhancement could make fossil-like systems more efficient strong gravitational lenses. Since gravitational lensing also preferentially selects merging systems along the line of sight, it follows that targeting systems with strong gravitational arcs nearby could be a more efficient way of locating fossil systems and their progenitors. Kanagusuku et al. (2016) found that in the Millennium Simulation most of today’s fossils became fossils between $0.3 < z < 0.6$, which happens to be the optimal distance to observe groups that act as strong lenses (Trentham 1995). This motivates us to select our sample from the CAMbridge Sloan Survey of Wide ARcs in the Sky (CASSOWARY) catalog (Belokurov et al. 2009; Stark et al. 2013), which searches for strong gravitational arcs in the Sloan Digital Sky Survey (SDSS) and has an average lens redshift of $z \sim 0.4$. Our goals in this study are to identify more examples of fossil progenitors (such as the Cheshire Cat) in the CASSOWARY catalog using SDSS photometry, form a catalog of these progenitors, and contrast their properties against fossil and nonfossil systems. A control set of near-identical, nonlensing galaxy groups will also be analyzed to see whether the presence of a strong gravitational arc near a group biases it toward being a fossil system. We present results from our analysis of all 58 CASSOWARY members, along with average cumulative luminosity functions for each category (fossil, progenitor, and normal systems).

In Section 2, we discuss the selection criteria for our sample from the SDSS archive, group scaling relations involved in determining each group’s physical parameters, how fossil status is determined, and how average luminosity functions were generated. Section 3 presents our catalog of lensing fossil systems and potential fossil progenitor systems and compares the results against a control sample of near-identical, nonlensing galaxy groups. In Section 4, we propose a possible fossil system formation time line using data from SDSS, incorporating fossil progenitors at varying stages of BCG/BGG formation. Section 5 summarizes our findings. We adopt the standard Λ CDM cosmology with $H_0 = 70 \text{ km s}^{-1} \text{ Mpc}^{-1}$ and $\Omega_M = 0.286$ throughout this work.

2. Sloan Data Analysis

2.1. Selection Criteria

The CASSOWARY catalog (Belokurov et al. 2009; Stark et al. 2013) identified strong gravitational arcs in the SDSS DR7 archive

¹⁰ It is important to note that it is logically possible for a BGG/BCG to be extremely efficient at turning gas into stars, essentially preventing any other large galaxies from forming in the group/cluster. Fossil systems formed via this channel would simply be “born that way”; however, our data cannot distinguish between this process and early dry mergers.

by searching for blue companions or arcs separated from a luminous red galaxy by $\sim 3''$. To date, 58 lensing systems have been identified, with many having been confirmed via spectroscopic observations of both the lensing and lensed galaxies, with typical lensing galaxies lying between $0.2 < z < 0.7$ and lensed galaxies beyond $z \sim 1.5$. While it was not required that the lens be a galaxy group, it was found that most were. Moreover, many of the CASSOWARY groups were not previously identified in group catalogs, as they generally have few members and their higher redshifts create difficulties for automated selection techniques.

Our analysis primarily used SDSS DR12 photometric data, which consist of over 100 million cataloged sources observed in the *ugriz* bands that span over one-quarter of the sky. Unfortunately, due to the vastness of the data set, only the brightest galaxies have available spectra, limiting our ability to know precise distances and therefore accurate group membership. We therefore use photometric redshifts (photoZ) estimates provided in the SDSS archive, which are found using the observed colors of the sources, and correlate them to a database of spectroscopic redshifts (specZ) of galaxies of similar colors. This method allows for an estimate of the source's distance, bearing in mind that improvements could be made once a spectrum is taken.

It is important to note where the uncertainties in SDSS's photoZ measures come from and how they can be minimized. The error in the photoZ estimate directly correlates with the errors in the source's colors, meaning that the fainter sources have less accurate corresponding photoZ. Normally, at the distances of our targets, solely relying on photoZ to determine group membership is not optimal, so we developed a technique to construct reliable photoZ cuts for the other groups without spectroscopic information. *Gemini* GMOS optical spectroscopic redshifts for 48 galaxies for the Cheshire Cat (also a CASSOWARY object known as CSWA 2) were available (Irwin et al. 2015), along with supplemental redshifts found in the literature; these allowed us to confidently determine group membership. We therefore chose to use this group to construct our photometric inclusion criteria for the other CASSOWARY catalog systems. By querying SDSS for all available photoZs of each confirmed member of CSWA 2 along with their errors (18 were too faint for SDSS to estimate any photoZ) and comparing them to each specZ, we determined that a 2σ inclusion window about the BGG's specZ was sufficient to include all but the dimmest members (Figure 1).

In order to count red-sequence (or red-ridge) elliptical galaxies for use in group scaling relations, we incorporate a series of color cuts to exclude blue, late-type galaxies, as well as any red-ridge ellipticals at the wrong redshift. The average redshift of the CASSOWARY groups, combined with most CASSOWARY member galaxies being red-ridge ellipticals, drove us to omit the *u* band; the SDSS *u*-band errors were large for even the brightest BGG in our sample, suggesting that including the *u* band would add little information to our analysis. Thus, every color combination using the *griz* bands was inspected for the confirmed Cheshire Cat member galaxies. The tightest groupings would limit the number of interlopers being accidentally counted among the red-ridge elliptical members (Figure 2). Four parallelograms in color-color space were chosen and are displayed in Table 1. Galaxies outside any parallelogram are excluded. These two criteria were used to determine group membership status for the rest of the CASSOWARY catalog. The lack of spectra for each group

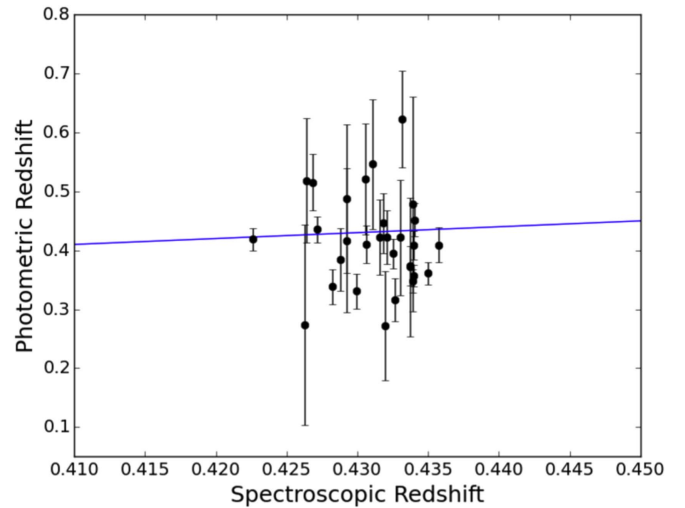


Figure 1. All specZ confirmed members of CSWA 2 that also had photoZ estimates available in SDSS (some were too faint). The blue line shows an ideal one-to-one relationship between specZ and photoZ.

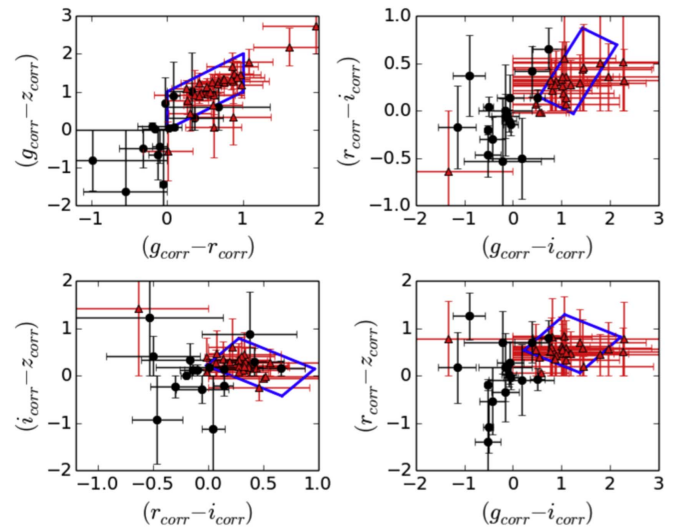


Figure 2. Four color-color group inclusion parallelograms created for the Cheshire Cat (CSWA 2) for red-ridge ellipticals; *K*-corrections and stellar evolutionary corrections have been included. Red triangles show confirmed member galaxies, and black circles show interlopers. Error bars were calculated quadratically from the reported SDSS DR12 magnitude errors. Confirmed member galaxies outside the regions are very faint and were only confirmed via spectroscopic redshifts.

means that when using these cuts the results will not be pure; however, statistically they are complete.

To account for the relatively high redshift of the CASSOWARY groups, *K*-corrections for groups of $z < 0.5$ were found using the “*K*-corrections Calculator” (Chilingarian et al. 2010).¹¹ For groups with $z > 0.5$, *K*-corrections were estimated using $D_n 4000$ measures (Westra et al. 2010) assuming a typical elliptical galaxy $D_n 4000 \sim 1.65$. Stellar evolutionary corrections for the *griz* bands were taken from Roche et al. (2009). Finally, we imposed a corrected *i*-band magnitude limit of $m_i < 20.84$ to find N_{200} , defined as the number of red-ridge ellipticals with $L_{\text{gal}} > 0.4L^*$ inside the group's virial radius, taken to be R_{200} (Wiesner et al. 2012).

¹¹ <http://kcor.sai.msu.ru/>

Table 1

Equations for Lines Used to Build Parallelograms in Color Space to Exclude All Galaxies except Red-ridge Ellipticals Useful for Group Scaling Relations, with Each Inclusion Region Denoted by R1, R2, R3, and R4

	Cut 1	Cut 2	Cut 3	Cut 4
R1	$(g - z) > -3.63(g - r) + 3.0$	$(g - z) < 1.05(g - r) + 1.11$	$(g - z) < -3.63(g - r) + 7.45$	$(g - z) > 1.05(g - r) + 0.35$
R2	$(r - i) > -0.25(g - i) + 0.28$	$(r - i) < 0.81(g - i) - 0.29$	$(r - i) < -0.25(g - i) + 1.23$	$(r - i) > 0.81(g - i) - 1.04$
R3	$(i - z) > -0.94(r - i) + 0.20$	$(i - z) < 1.95(r - i) + 0.25$	$(i - z) < -0.94(r - i) + 1.05$	$(i - z) > 1.95(r - i) - 1.73$
R4	$(r - z) > -0.41(g - i) + 0.63$	$(r - z) < 0.90(g - i) + 0.33$	$(r - z) < -0.41(g - i) + 1.73$	$(r - z) > 0.90(g - i) - 1.18$

Note. K -corrections and stellar evolutionary corrections are included to bring galaxies to a $z = 0$ frame.

In order to find each group’s R_{200} and other physical properties, we adopted an iterative process using group scaling relations involving N_{200} in Lopes et al. (2009),

$$\ln(R_{200}) = 0.05 + 0.39 \ln\left(\frac{N_{200}}{25}\right) h_{70}^{-1} \text{ Mpc} \quad (1)$$

$$\ln(M_{200}) = 0.21 + 0.83 \ln\left(\frac{N_{200}}{25}\right) h_{70}^{-1} M_{\odot}. \quad (2)$$

We first adopted a characteristic R_{200} of 1 Mpc as a starting point. This size was used in an SDSS query to extract all galaxies within the circular angular region. These galaxies were analyzed using our color/photoZ selection criteria, which gave us a preliminary value for that system’s N_{200} . To deal with any remaining interlopers present within the extraction region, which could slightly inflate N_{200} and consequently R_{200} , we took eight regions of angular size equal to the group’s current R_{200} immediately adjacent to the target group and applied the same selection process to the galaxies within these regions. We averaged these eight results together to obtain an expected $N_{200}^{\text{interloper}}$ for each group based on the group’s location in the sky. This value was subtracted from the group’s N_{200} to arrive at a more accurate richness. The new N_{200} was used to calculate a new R_{200} , and the process was repeated until a single value for N_{200} and R_{200} was converged upon. By using this method, we were able to agree with other SDSS galaxy cluster richness catalogs (Wen et al. 2012) on N_{200} to within 10% for the 17 groups with existing N_{200} estimates. Errors in galaxy colors were dealt with by adding in quadrature, and if a galaxy’s color error bars pushed it into the inclusion regions, it was counted as a potential group member; this only significantly changes results in the most distant groups.

2.2. Determining Fossil Status

With color cuts, photometric redshift cuts, galaxy interloper averages, and reliable R_{200} estimates in hand, we constructed galaxy membership catalogs for all 58 CASSOWARY members. At this point, we checked the fossil status of each group using both the Jones et al. (2003) criteria of $\Delta m_{12} \geq 2.0$ and the Dariush et al. (2010) criteria of $\Delta m_{14} \geq 2.5$; systems that satisfied the optical criteria as is were labeled as fossil systems. Groups that were not classified as fossil systems moved on to the next stage of analysis to determine whether they are fossil progenitors.

Taking the brightest galaxy as the center of the system, we calculated the projected separation of all members from the BGG, along with their masses (assuming a mass-to-light ratio of 6 in the r band). We took this information and calculated an expected timescale for the galaxy to merge with the BGG for

each member using $T_{\text{merge}} \approx 1.6rM_*^{-0.3}$ Gyr, where r is the maximum projected separation of the galaxies in units of $35.7h_{0.7}^{-1}$ kpc and M_* is the sum of the galaxies’ masses in units of $4.3 \times 10^{11}h_{0.7}^{-1}M_{\odot}$ (Kitzbichler & White 2008). We adopt this timescale since it likely overpredicts the merger time by a factor of two relative to other methods (Kitzbichler & White 2008), ensuring that the merger is most likely completed in the specified timescale. Based on the group’s look-back time, we determined which member galaxies had sufficient time to be cannibalized by the BGG and their luminosities added to the BGG. Using this “new” BGG luminosity, the fossil status of each group was again checked; if a group became a fossil via this process, it was labeled as a fossil progenitor. Finally, all groups that still did not meet either fossil criterion were labeled for this work as normal groups, as no amount of possible merging could build a large enough BGG for these groups to transition into fossil groups by $z = 0$ (Table 2).

2.3. Luminosity Functions

Once all 58 CASSOWARY catalog members were sorted based on their fossil status, we converted galaxy apparent r -band magnitudes (m_r) into absolute magnitudes (M_r) using

$$M_r = m_r - 25 - 5 \log\left(\frac{D_L}{1 \text{ Mpc}}\right) - K_r - 0.85z, \quad (3)$$

where D_L is the luminosity distance to the group, K_r is the r -band K -correction, and the last term is the stellar evolutionary correction involving the group’s redshift (Roche et al. 2009). We then generated three average luminosity functions (one for fossils, one for progenitors, and one for normal groups) using all the member galaxies for each category. Due to the low galaxy count in the brightest bins of the average luminosity functions, errors in galaxy count were handled using Poisson statistics with $\sigma \approx 1 + (n + 0.75)^{1/2}$, where n is the number of member galaxies within the luminosity bin (Gehrels 1986).

3. Discussion

3.1. CASSOWARY Strong-lensing Sample

Of the 58 CASSOWARY members, it was found that six are most likely large, lone ellipticals (possessing an $N_{200} < 5$) that happen to act as strong gravitational lenses and were not included in any luminosity functions or fossil/progenitor fractions. Of the remaining 52 strong-lensing systems, we found that $13.5\% \pm 2.8\%$ are¹² Jones fossils ($\Delta m_{12} \geq 2.0$) and $17.3\% \pm 2.6\%$ are Dariush fossils ($\Delta m_{14} \geq 2.5$), consistent

¹² Errors are reported at 1σ confidence.

Table 2
Fossil Status of All CASSOWARY Members

Name	R.A., Decl. (deg)	z_{spec} (BGG)	$L_{\text{BGG}} \times 10^{11} L_{\odot}$	$D_{\text{off}}^{\text{BGG}}$ (kpc)	N_{200}	$M_{200} \times 10^{14} M_{\odot}$	$P_J/P_D/F_J/F_D$	$\Delta m_{12} \Delta m_{14}$	$\Delta m_{12}^{\text{merge}} \Delta m_{14}^{\text{merge}}$	t_{merge} (Gyr)
CSWA 1	177.1381 19.5008	0.444	3.41	1.17	5	0.32	x/x/✓/x	2.3 2.4		
CSWA 2	159.6816 48.8216	0.426	3.84	13.31	10	0.58	✓/✓/✓/✓	0.2 2.4	3.3 3.7	0.9
CSWA 3	190.1345 45.1508	0.273	1.14	14.91	12	0.67	x/x/x/x	0.2 1.4		
CSWA 4	135.3432 18.2423	0.346	4.38	14.15	32	1.52	x/x/x/✓	1.4 3.1		
CSWA 5	191.2126 1.4122	0.388	2.33	59.30	14	0.78	x/✓/x/x	0.2 1.6	1.9 2.9	4.1
CSWA 6	181.5087 51.7082	0.422	4.60	0.42	18	0.94	x/x/✓/✓	2.2 2.8		
CSWA 7	174.4169 49.6099	0.448	2.29	0.84	20	1.05	x/x/x/x	1.0 1.2		
CSWA 8	182.3487 26.6796	0.558	4.68	3.05	61	2.60	x/x/x/x	1.6 2.2		
CSWA 9	186.8281 17.4311	0.298	2.84	11.91	23	1.16	x/x/x/x	0.7 1.9		
CSWA 10	339.6305 13.3322	0.413	5.99	2.26	30	1.43	x/✓/x/x	1.4 2.2	1.9 2.8	3.9
CSWA 11	120.0544 8.4023	0.314	3.53	16.25	26	1.28	x/x/✓/x	2.0 2.1		
CSWA 12	173.3049 50.1445	0.394	3.22	7.91	45	2.00	x/x/x/x	0.7 1.4		
CSWA 13	189.4008 55.5619	0.410	2.58	7.18	26	1.27	x/x/x/x	0.4 1.8		
CSWA 14	260.9007 34.1995	0.442	5.33	4.57	18	0.93	✓/✓/✓/✓	0.6 1.9	2.5 2.8	3.6
CSWA 15	152.2491 19.6215	0.306	4.36	21.72	51	2.24	x/x/x/x	0.3 1.6		
CSWA 16	167.7653 53.1486	0.413	3.60	10.49	79	3.20	x/x/x/x	0.1 1.1		
CSWA 17	174.5373 27.9085	0.345	1.81	9.04	74	3.04	x/x/x/x	1.3 1.4		
CSWA 18	173.5281 25.5598	0.070	1.32	11.13 ^a	25	1.25	x/x/x/x	1.1 2.0		
CSWA 19	135.0110 22.5680	0.489	0.78	6.67	17	0.89	x/x/x/x	0.6 0.8		
CSWA 20	220.4548 14.6890	0.741	4.20	3.20	1	0.09	x/x/x/x			
CSWA 21	5.6705 14.5196	0.381	2.86	1.53	28	1.36	x/x/x/x	1.0 1.3		
CSWA 22	26.7334 -9.4979	0.447	6.69	3.27	60	2.56	x/x/x/x	1.1 1.8		
CSWA 23	126.8701 22.5483	0.335	5.31	43.49	88	3.49	x/x/x/x	1.1 1.5		
CSWA 24	227.8281 47.2279	0.451	5.10	4.34	13	0.71	✓/✓/✓/✓	2.0 ^b 2.6 ^b	2.1 2.7	2.2
CSWA 25	162.4298 44.3432	0.230	2.37	6.18	50	2.21	x/x/x/x	1.3 1.6		
CSWA 26	168.2944 23.9443	0.336	11.38	5.40	83	3.35	✓/x/x/✓	1.5 2.5	2.9 3.4	2.1
CSWA 27	247.4773 35.4776	0.170	0.83	0.85	63	2.66	x/x/x/x	0.2 0.7		
CSWA 28	205.8869 41.9176	0.418	5.25	24.25	31	1.48	✓/✓/✓/✓	1.8 2.3	2.1 2.8	1.6
CSWA 29	130.0877 10.8702	0.247	0.88	15.27	2	0.18	x/x/x/x			
CSWA 30	132.8604 35.9705	0.272	2.97	10.82	31	1.46	x/✓/x/x	0.7 2.2	1.1 2.6	2.0
CSWA 31	140.3573 18.1715	0.683	18.11	4.89	5	0.32	x/x/✓/x	2.1^c		
CSWA 32	153.7740 55.5051	0.204	1.21	1.24	1	0.09	x/x/x/x			
CSWA 33	162.3475 35.7447	0.332	3.46	6.79	26	1.26	x/x/x/x	1.0 2.4		
CSWA 34	4.2564 -10.1531	0.501	0.67	17.33	3	0.19	x/x/x/x			
CSWA 35	149.4133 5.1589	0.447	2.15	27.51	9	0.52	x/x/x/x	1.1 1.3		
CSWA 36	181.8996 52.9165	0.266	1.30	^d	26	1.25	x/✓/x/x	0.4 1.3	0.6/ 2.6	3.0
CSWA 37	199.5480 39.7075	0.475	4.90	10.73	19	0.98	✓/✓/✓/✓	0.8 1.7	3.0 3.3	3.5
CSWA 38	186.7154 21.8737	0.434	2.15	10.45	167	5.97	x/x/x/x	1.1/1.4		
CSWA 39	231.9376 6.8761	0.394	2.22	67.08	98	3.83	x/x/x/x	0.3/0.4		
CSWA 40	148.1676 34.5795	0.402	2.08	5.38	77	3.13	x/x/x/x	0.1/0.3		
CSWA 41	222.6277 39.1386	0.289	2.58	9.57	20	1.03	x/x/✓/✓	2.2 2.7		
CSWA 102	14.7039 -7.3660	0.639	16.77	16.50	5	0.30	x/x/✓/✓	2.5 ...		
CSWA 103	26.2679 -4.9311	0.633	8.67	0.54	4	0.27	x/x/x/x			
CSWA 104	167.5738 64.9965	0.659	9.12	30.32	2	0.12	x/x/x/x			
CSWA 105	168.7683 16.7606	0.537	2.43	57.01	7	0.41	✓/✓/✓/✓	0.9 1.8	2.8 ...	4.7
CSWA 107	176.8471 33.5314	0.212	1.99	27.72	41	1.85	x/x/x/x	0.9 1.5		
CSWA 108	179.0228 19.1868	0.545	3.35	15.39	13	0.70	x/x/x/x	1.1 1.4		
CSWA 111	345.0719 22.2249	0.443	3.89	15.36	25	1.23	x/x/x/x	1.1 1.6		
CSWA 116	25.9589 16.1274	0.415	2.18	3.05	7	0.85	✓/x/x/x	1.9 2.2	2.9 3.4	2.0
CSWA 117	150.5106 60.3404	0.571	3.25	23.42	30	1.44	x/✓/x/x	0.8 1.6	1.9 2.7	3.4
CSWA 128	299.6473 59.8495	0.214	4.60	7.60	42	1.90	x/✓/✓/✓	2.0 2.3	2.1 2.7	1.9
CSWA 139	121.8814 44.1800	0.449	2.07	5.26	8	0.45	✓/✓/✓/✓	0.8 2.0	2.6 ...	3.4
CSWA 141	131.6977 4.7680	0.241	1.89	4.57	22	1.11	✓/x/x/x	1.4/1.8	2.0 2.4	0.6
CSWA 142	133.6197 10.1373	0.298	2.10	6.66	54	2.34	✓/✓/✓/✓	0.6 1.2	2.1 3.1	2.9
CSWA 159	335.5358 27.7596	0.485	4.76	8.04	6	0.36	✓/x/x/✓	1.3 2.8	3.6
CSWA 163	329.6820 2.9584	0.287	2.37	4.91	18	0.93	x/✓/x/x	1.4 2.1	1.8 2.7	3.2
CSWA 164	38.2078 -3.3906	0.450	6.27	1.08	10	0.55	x/x/x/✓	1.7 3.2		
CSWA 165	16.3318 1.7489	0.361	2.80	6.76	14	0.78	x/x/x/✓	1.7 2.8		

Notes. All 58 CASSOWARY members and their general properties, with $D_{\text{off}}^{\text{BGG}}$ indicating the BGG offset from the lensing center of mass. Since both Jones et al. (2003) and Dariush et al. (2010) criteria were used to determine fossil status, we include the magnitude gap in the r band between the first- and second-rank galaxies (Δm_{12}) and between the first- and fourth-rank galaxies (Δm_{14}) within $0.5R_{200}$. The $P_{J/D}$ and $F_{J/D}$ columns were added to differentiate between Jones(J)/Dariush(D) progenitors or fossils, respectively. Entries in boldface indicate optical fossil status being reached either now or after merging is completed. Dashes under the merged column indicate all galaxies within $0.5R_{200}$ merging into one BGG by $z = 0$. t_{merge} indicates the expected merger timescale from Kitzbichler & White's (2008) relation until fossil status is achieved.

^a No spectra available for source galaxy; lensing confirmation needed.

^b Double nucleus detected in archival *HST* imaging negating fossil status until merging is finished.

^c *Gemini* GMOS data from Grillo et al. (2013).

^d The geometry of CSWA 36 prevents the arc from being easily fit, and thus no offset was measured.

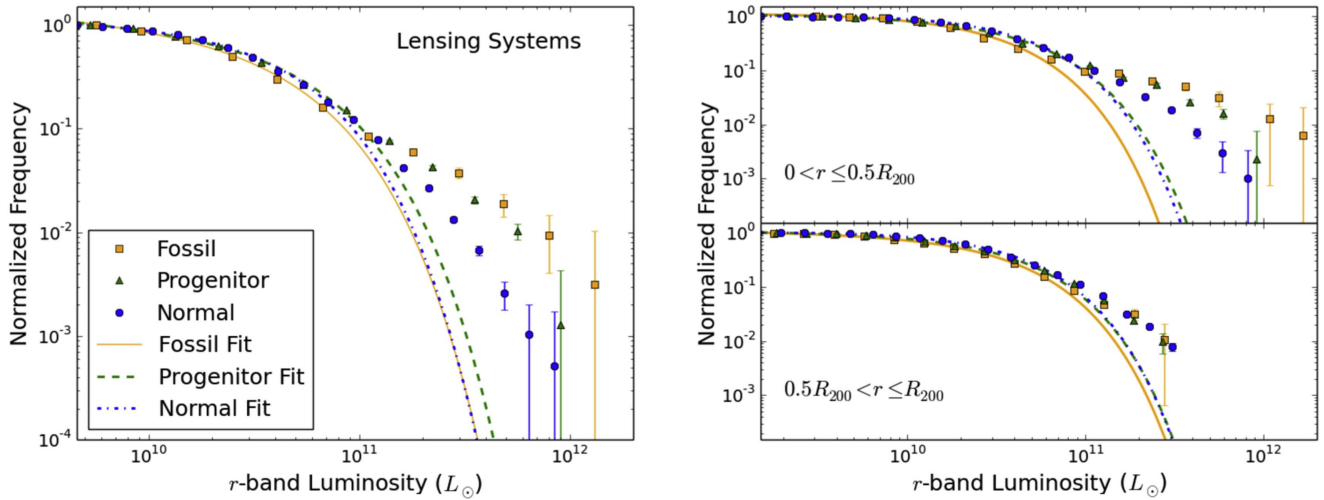


Figure 3. Left: cumulative luminosity functions of CASSOWARY systems separated by classification—normal, progenitor, and fossil. The curves represent the best-fit Schechter function found using least-squares fitting for each population excluding the BGGs. The progenitor function falls between the normal and fossil functions at the bright end ($L \gtrsim 10^{11} L_{\odot}$), supporting the idea that fossil progenitors are a bridge between normal and fossil systems. Right: same luminosity functions binned by inner- and outer-half virial radii. The inner regions exaggerate differences between the three populations, which may be due to frequent mergers/interactions of members. The outer regions show little statistical difference from one another; however, as a whole, the outer members possess more bright galaxies than the best-fit model would suggest. Error bars are at 1σ .

with the expected 8%–20% fossil system rate for randomly selected groups within $z < 0.2$ (Jones et al. 2003). We found that $23.1\% \pm 2.5\%$ of the CASSOWARY systems are Jones fossil progenitors and $28.9\% \pm 2.5\%$ are Dariush fossil progenitors. This higher rate of fossil progenitors in the CASSOWARY sample is not surprising considering that Kanagusuku et al. (2016) found that in the Millennium Simulation systems that were fossils at $z = 0$ finished forming their BGG (creating the required $\Delta m_{12}/\Delta m_{14}$ r -band magnitude gap) between $0.3 < z < 0.6$ on average. Since the average redshift of the CASSOWARY members is $z \sim 0.4$, we expect to see a collection of near-fossil systems, as we are seeing analogs to today’s fossil systems in midcannibalization of their L^* members. An interesting thing to note is that if one assumes that *all* the CASSOWARY progenitors and fossils become/stay fossils, one arrives at a $z = 0$ Jones fossil percentage of $36.6\% \pm 2.4\%$ and a Dariush percentage of $46.1\% \pm 2.3\%$; this implies that we should see far more nearby fossil systems than we currently do. One explanation why we do not see such an overabundance of nearby fossils is that fossils are transitory in nature, and the look-back time is long enough to allow some bright galaxies to fall within half of the fossil’s virial radius, thereby breaking the fossil’s status. Another explanation is that in the CASSOWARY strong-lensing sample we are seeing a subset of systems that are more likely to be fossil systems; these two hypotheses will be explored further in the nonlensing control sample section.

To better determine whether we are truly seeing the progenitors of today’s fossil systems, we contrasted the galaxy luminosity functions of each category against one another, as fossil system luminosity functions show a clear deficit in L^* members when compared to comparable-sized normal groups and clusters (Gozaliasl et al. 2014). Fossil progenitors might be expected to be a transitional step between the two extremes, losing L^* galaxies as they are consumed by the BCGs. We created three average cumulative galaxy luminosity functions (a fossil, progenitor, and normal function) from the CASSOWARY lensing sample to ensure that we were comparing strong-lensing

systems to other strong-lensing systems.¹³ Due to the large amount of overlap between the two prevailing fossil criteria (Jones/Dariush) in this sample, the cumulative luminosity functions combined both Jones and Dariush fossils/progenitors to minimize errors. It is important to note that the poor fitting at the bright end is due to the “BCG bump,” a known artifact of galaxy mergers in the centers of clusters and groups (Hansen et al. 2005). Excluding the BGGs, we found that overall the lensing fossil and normal population fits are nearly identical. However, when the BGGs are introduced into the data set, we found that the fossil luminosity function greatly diverged from the normal luminosity function at the bright end, as expected (Figure 3). The progenitor luminosity function matched the normal function at the faint end. However, the progenitor function fell between the normal and fossil functions at the bright end, suggesting that fossil progenitors are currently losing their intermediate members while gaining very bright members, thereby moving the groups closer to fossil status. This supports the notion that fossil systems form their massive BCGs via cannibalization of intermediate-mass member galaxies. SDSS images of the inner regions of groups classified as fossil progenitors also very often show an extremely crowded environment near the BCG, further supporting this mechanism of fossil formation (Figure 6).

We also find that while many CASSOWARY systems visually appear to be compact groups, none reach the compactness criteria of a $\mu_G < 26.0$ surface brightness in the smallest circle that includes at least three galaxies within 3 mag of the BGG (Hickson 1982), making none of our systems compact groups. This supports the findings of Farhang et al. (2017) in the Millennium Simulation, where only $3\% \pm 2\%$ of fossil systems were simultaneously compact groups. The fact that none of the 12 Jones progenitors in our $0.2 < z < 0.7$ sample were compact groups contrasts their estimates of $36\% \pm 2\%$ of fossil progenitors being identified as a compact

¹³ In the cases of split identification (e.g., Jones fossil and Dariush progenitor), the Jones criterion was chosen for forming the luminosity functions since it is the most widely cited.

group between $0 < z < 1.0$. We hesitate to place our own numerical constraints on this fraction, as our sample varies greatly from theirs and we believe it is not large enough to show any meaningful correlations on its own.

Much work has been done investigating the global deficit in intermediate-luminosity members and the value/evolution of the faint-end slope of the fossil luminosity function, finding that the deficit in L^* members is likely due to cannibalization by the BCG and the faint-end slope is consistent with normal groups (Lieder et al. 2013; Gozaliasl et al. 2014; Zarattini et al. 2015). However, little work has gone toward investigating fossil populations in different radial bins, where initial group conditions could still be encoded (particularly in the outer regions). Binning the average luminosity functions into inner ($r \leq 0.5R_{200}$) and outer ($0.5R_{200} < r \leq R_{200}$) regions reveals that this deficit in intermediate-mass galaxies/abundance of extremely bright galaxies in fossil progenitors and fossil systems is exaggerated for $r \leq 0.5R_{200}$ (Figure 3, right panel). This is likely due to the increased galaxy density near the center effectively speeding up the galaxy interaction rate; therefore, the central regions of fossil or near-fossil systems should show the most extreme differences from nonfossils. While the inner progenitor fit is nearly identical to the normal fit, when the BGGs are included in the histogram a clear difference can be seen, placing it firmly between the normal and fossil functions.

We quantified the statistical significance of these differences between data sets via a one-sided Kolmogorov–Smirnov (K-S) test, which gives the probability that differing data sets come from the same cumulative distribution function. For $0 < r \leq 0.5R_{200}$, even with the relative lack of data points, lensing fossil systems showed only a 0.84% chance of being identical to normal lensing systems. Due to a larger sample size, lensing progenitors also proved to be significantly different from normal lensing systems, with only a 0.01% chance of being identical within $r \leq 0.5R_{200}$. Unfortunately, due to insufficient galaxy counts in the lensing fossil population, we were not able to find a significant difference between lensing fossils and progenitors. The outer-half virial radius galaxies showed no statistically significant differences between the populations, suggesting that most differences in galaxy populations for fossil systems exist near the center, where the most processing has occurred. However, all lensing systems exhibit an average $\sim 2\sigma$ deviation from a Schechter function in the outer $0.5R_{200}$ for galaxies brighter than L^* , which is surprising. Since these galaxies are farther away from the center, one would expect them to be much less processed and therefore be better represented by the fits. Additionally, there are no BGGs in the outer regions to skew the data away from a Schechter function. While by no means definitive, this suggests that lensing systems may form differently from nonlensing systems of comparable mass.

A consequence of the CASSOWARY systems acting as strong lenses is that we have a convenient and independent way to locate the center of mass of the inner regions of each group, which can help shed light on the supposed relaxed nature of fossils. The difference between this lensing center of mass and the luminosity centroid of the BGG offers information regarding the age of the group, with large offsets implying a younger system (Raouf et al. 2014). On average, we see normal, progenitor, and fossil system BGG offsets of 13.5 ± 2.6 kpc, 14.6 ± 4.3 kpc, and 7.8 ± 2.0 kpc, respectively. Immediately apparent is the smaller

offset fossils have compared to other systems; this supports the idea of fossils being more relaxed (and possibly older) than nonfossils on average. Also noticeable is the high offset and wide spread in progenitor BGGs, which could be partially explained by their disturbed nature evident in images and range of fossil transition timescales. Since the progenitor BGG offset is consistent with the normal BGG offset, one cannot say on average that progenitors are older or younger than normal systems; a case-by-case analysis would be needed.

3.2. Nonlensing Control Sample

All members of our sample exhibit strong gravitational arcs near the BGGs, implying a high central mass concentration for these systems. To see how/if the presence of strong gravitational arcs biases our fossil system and progenitor findings, we assembled a one-to-one random control sample of nonlensing groups from the Augmented maxBCG cluster catalog (Rykoff et al. 2012), Clusters of galaxies in SDSS-III (Wen et al. 2012), and Richness of Galaxy Clusters (Oguri 2014) catalogs. Control groups were selected to match (within 10%) each CASSOWARY group in both redshift and galaxy richness, and when multiple matches for control groups were found among the catalogs, the closest match was chosen. To increase the accuracy of this one-to-one comparison, we found two nonlensing matches for each CASSOWARY group.¹⁴ To ensure that our nonlensing control sample’s halo properties matched as closely as possible to the CASSOWARY groups, we compared each control group’s stellar luminosity against its lensing counterpart’s; this can be used as a proxy for a system’s stellar mass in M_* – M_{halo} relations. The average scatter in M_* for a given M_{halo} is a factor of 1.4 (Behroozi et al. 2010); we measure a factor of 1.1 scatter in our sample. This means that we are limited by the scatter inherent in the relation and not our sample (Figure 4).

Using the same photoZ and color cuts as the lensing sample, we found fossil percentages of $2.9\% \pm 1.6\%$ (Jones) and $13.6\% \pm 1.2\%$ (Dariush) and fossil progenitor percentages of $17.5\% \pm 1.2\%$ (Jones) and $25.2\% \pm 1.1\%$ (Dariush), showing that while being a strong gravitational lens does not significantly alter the Dariush fossil fraction, it does greatly improve the chances that a fossil will be a classic Jones fossil. The progenitor fraction is consistent between the control sample and lensing sample, suggesting that in general the progenitor fraction is not greatly affected by the presence of gravitational arcs. We note that while the nonlensing Dariush fossil fraction is consistent with previous findings (Jones et al. 2003; Gozaliasl et al. 2014 for $z \leq 0.6$; Trevisan et al. 2017), our nonlensing Jones fossil fraction of $2.9\% \pm 1.6\%$ is below their estimates of 8%–20%, $22\% \pm 6\%$, and $\sim 10\%$, respectively. This could be partially due to the Gozaliasl et al. (2014) $\Delta m_{12} \geq 1.7$ criterion being less restrictive than the classical Jones et al. (2003) $\Delta m_{12} \geq 2.0$. However, we stress that their samples included nearby ($z < 0.25$, $z \leq 0.6$, and $z < 0.07$) groups; we are probing a different epoch (upward of 3 Gyr of available time for group evolution) by excluding the redshift range where most fossils are seen today. This, combined with the knowledge that most of today’s fossils began BGG assembly between $0.3 < z < 0.6$ (Kanagasaki

¹⁴ Only one nonlensing match was able to be found for CSWA 31 and CSWA 102 owing to their high redshifts ($z = 0.683$ and $z = 0.639$) and poor member count ($N_{200} = 5$).

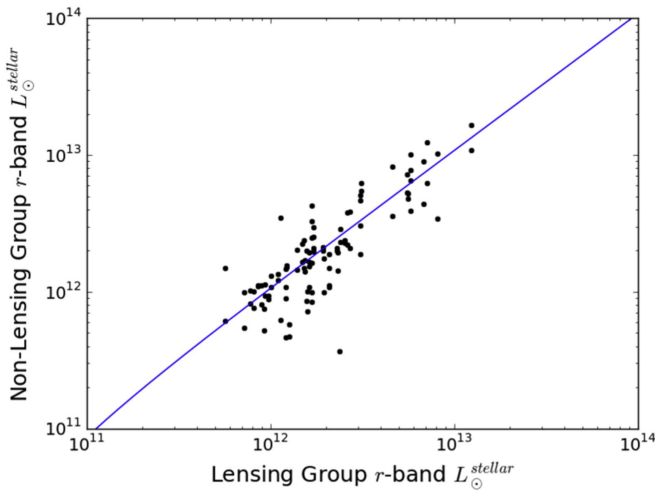


Figure 4. Comparing the group stellar luminosities, as a proxy for stellar mass, of the nonlensing control groups vs. their lensing counterparts to see how well the average halo properties of each sample match. We find a best fit of $L_{\odot}^{\text{Non-Lensing}} = 1.1 L_{\odot}^{\text{Lensing}} - 2.2 \times 10^{10} \text{ erg s}^{-1}$, which lies within the inherent scatter of the Behroozi et al. (2010) halo relation.

et al. 2016), helps explain why we see fewer fully formed fossils in our control sample.

To see whether the lower fossil occurrence rate in our sample could be due to inadvertently including too many bright interloper galaxies (since spectroscopic data are lacking for these groups), we calculated the bright galaxy ($L_{\odot} > 0.4L^*$) overdensity within each CASSOWARY group compared to the surrounding regions. In nonfossil CASSOWARY groups, an overdensity of bright galaxies (sufficient to prevent that group from being a fossil) within $0.5R_{200}$ was confirmed at 13σ confidence above the expected interloper value, indicating that our fossil fractions are reliable. The apparent fossil deficit could be accounted for owing to the redshift range of our sample ($0.2 < z < 0.7$). Since most fossils discovered lie near $z \sim 0.1$, and Kanagusuku et al. (2016) found in the Millennium Simulation that most $z = 0$ fossils made the transition between $0.3 < z < 0.6$, there could be a lower fossil fraction in our samples.

Average galaxy luminosity functions were also generated for the nonlensing sample to compare against the lensing sample to see how strong lensing might affect a group’s galaxy population (Figure 5). The nonlensing fossil and normal luminosity functions exhibit similar behavior to the lensing sample. Nonlensing fossils show a 0.01% chance of being identical to nonlensing normal and progenitor systems, confirming that on average fossil systems’ inner regions house a different population of galaxies than nonfossils. Interestingly, nonlensing progenitors showed virtually no differences from nonlensing normal systems at any radii; this reinforces our hypothesis that the presence of a strong gravitational arc marks the most extreme examples of fossil formation at all stages. Also, the nonlensing progenitor fit falls between the other two in each radial bin. Reintroducing the BGGs maintains this in-between state for the nonlensing progenitors. Applying the K-S test to the nonlensing populations showed again that significant differences only appear within $0 < r \leq 0.5R_{200}$.

3.3. Comparing Lensing versus Nonlensing Samples

A comparison of the lensed versus nonlensed fossil luminosity function revealed interesting distinctions; on average, lensing

fossil systems lack intermediate-mass galaxies and house larger BGGs than their nonlensing counterparts (Figure 6). While the latter is not terribly surprising (as larger galaxies are more likely to act as good gravitational lenses), the former offers help explaining why the lensing sample has significantly more Jones fossils than the nonlensing sample; the lensing sample is the extreme case in fossil formation. In CASSOWARY fossils (and progenitors to a lesser extent), we are seeing elevated L^* cannibalization, resulting in intermediate galaxy deficits and an overrepresentation of extremely bright galaxies. Comparing the nonlensing progenitor fit to its lensing counterpart reveals even sharper differences between nonlensing fossils and lensing fossils (top panels of Figure 6). On average, the lensing progenitors have fewer bright L^* galaxies than the nonlensing progenitors. This could be an indication of a strong-lensing selection bias. Since the presence of strong lensing indicates a high mass concentration, lensing progenitors could have already had most of their L^* members consumed by the BGGs.

Since Dariush fossils do not need such a large luminosity difference between the BGG and the next-ranked galaxies, the nonlensing control sample holds many more Dariush fossils than Jones fossils. The nonlensing control sample also indicates that while the presence of a strong gravitational arc does not strongly affect the likelihood of finding the progenitors to today’s fossils around $z \sim 0.4$, it does appear to greatly increase the probability of locating Jones fossil systems. Applying the K-S test, this time to lensing versus nonlensing systems, again shows significant differences only within $0.5R_{200}$. For the inner regions, normal systems proved to be consistent between lensing and nonlensing systems. Progenitors, on the other hand, showed a 0.01% chance of being identical; such a striking result means that a strong-lensing bias may very well exist. Since lensing progenitors on average show different galaxy populations than nonlensing progenitors, it can be inferred that the same (if not more) can be said for lensing versus nonlensing fossils. Unfortunately, errors in bin count for both fossil populations kept us from arriving at any meaningful result; this can be remedied by increasing the sample size.

When one compares the best-fit Schechter functions of lensing versus nonlensing systems as a whole, an interesting distinction is found: at every radial bin, systems acting as strong gravitational lenses exhibit an intermediate-luminosity member deficit regardless of fossil status. While this is expected near the center of most groups (the act of forming the BGG consumes many of these galaxies, thereby shifting L^* toward the faint end), this deficit supports the existence of a strong-lensing bias toward fossil-like systems. To test whether or not these lensing systems are preferentially selecting systems with different initial conditions from normal groups, thereby supporting the idea that some fossils are born differently than most systems, the outer regions must be probed to see whether the galaxy populations differ there as well. However, the overall lack of members in the outer-half virial radii of the systems made any conclusions statistically insignificant.

4. Progenitor—Fossil Properties, Time Lines, and the Longevity of Fossil Systems

Since we have many progenitors in the CASSOWARY catalog with a wide range of merging timescales until transitioning into a fossil system (Table 2), we can form a rough time line of today’s average fossil system’s formation process from its beginning, through the cannibalization phase

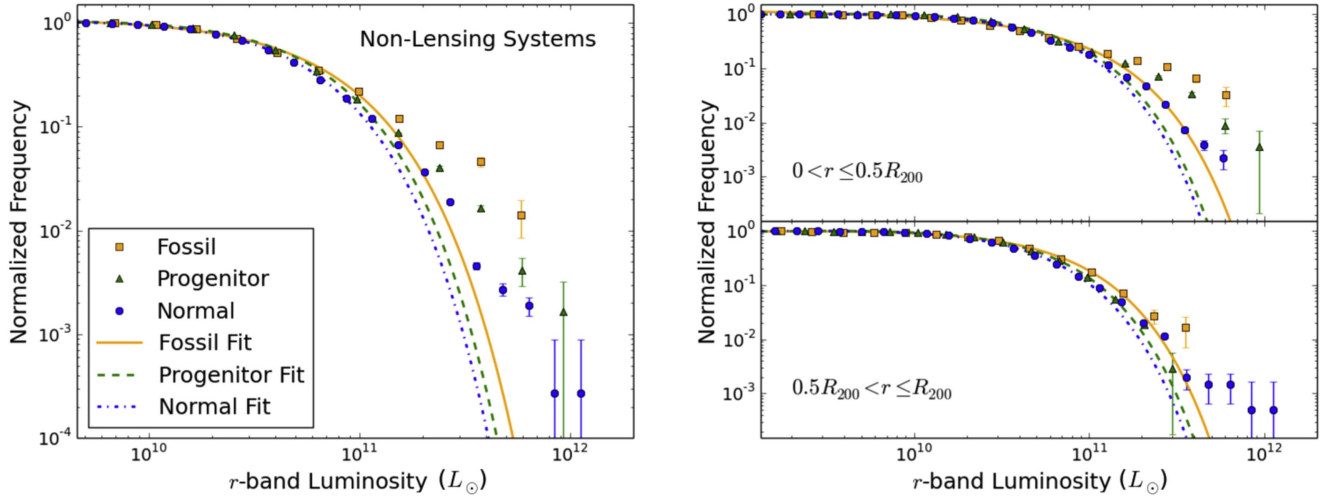


Figure 5. Left: cumulative luminosity functions of our nonlensing control sample for all member galaxies. For nonlensing groups, differences in the bright end (while still visually apparent) are not as prominent as our lensing systems, supporting the existence of a strong-lensing bias. Right: same nonlensing luminosity functions binned by inner- and outer-half virial radii. The inner regions for nonlensing fossils and progenitors also show the excess of bright member galaxies when compared to normal groups, though, again, less pronounced than in our lensing sample. The outer regions show virtually no difference between progenitors and normal groups, with fossils only housing a few more bright galaxies. Error bars are at 1σ .

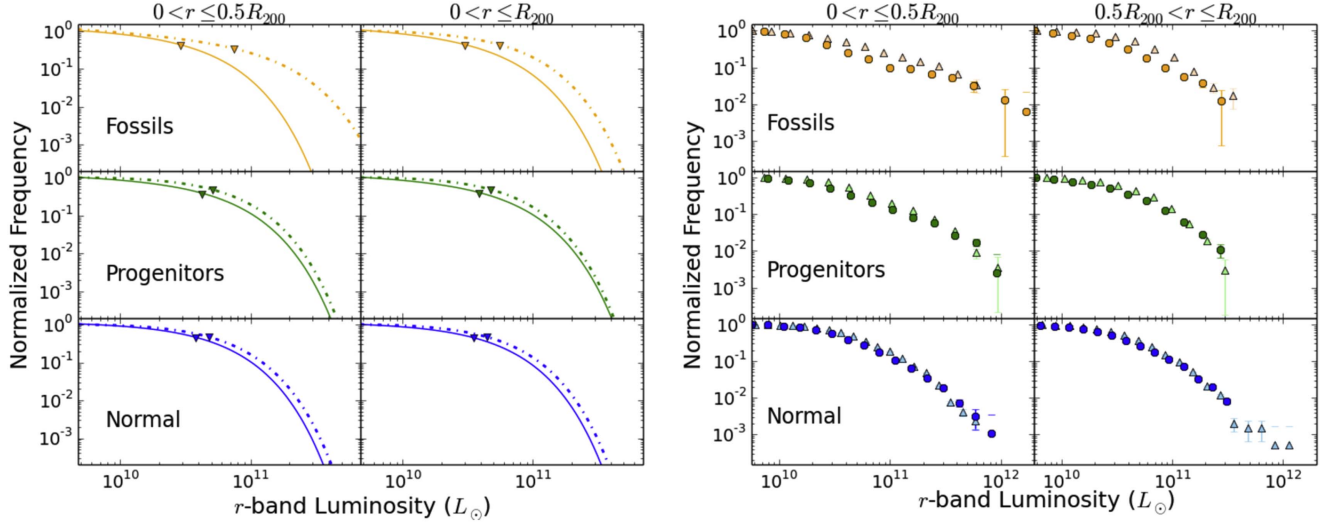


Figure 6. Left: contrasting the best-fit Schechter functions, excluding the BGGs, of lensing/nonlensing samples at inner-half and full virial radius bins separated by fossil status. The CSWA strong-lensing fit is shown with a solid line, and the nonlensing control fit is represented by the dashed line, with the derived L^* for each model marked. Right: galaxy member data taken from SDSS with BGGs included. Circles represent the lensing systems, and triangles mark the nonlensing systems. In each case, lensing groups show a deficit of intermediate-luminosity members and an excess in bright members, implying that lensing systems could be an example of the most extreme fossil systems, along with them being more likely to become fossils as opposed to similarly sized nonlensing systems.

building the large BGG, and finally concluding with a fossil system housing a large BGG and possessing a deficit in bright L^* galaxy members. To better illustrate the hypothesis of formation of a fossil system through the progenitor phase, we have assembled a collage of SDSS images from the CASSOWARY catalog (Figure 7). We order them to simulate the building of a fossil BGG via cannibalization of L^* members. Early in the progenitor phase, we expect there to be many bright galaxies present in the group and concentrated near the BGG, since dynamical friction has slowed the orbits of the largest galaxies and caused them to fall inward over the group's history. As time until fossil status is achieved shortens, more and more L^* galaxies will merge, with the BGG subsequently shifting the galaxy luminosity function of the group toward a fainter population, leaving only one or two

bright galaxies near the BGG. Once the last bright member merges with the BGG, a fossil system will form housing an elongated (possibly asymmetric) BGG. As the BGG begins to relax after the final major merger, it will eventually settle into a massive symmetric elliptical galaxy stereotypical of fossil systems. A follow-up study of progenitors is currently being done using *Chandra/Hubble Space Telescope (HST)* data to better see how the hot gas evolves alongside the stellar population as a group draws closer to the fossil threshold (L. Johnson et al. 2018, in preparation). We expect to see a correlation between a progenitor's X-ray properties and time until fossil status is achieved as well.

The high redshift of the CASSOWARY sample is beneficial for locating possible precursors to nearby fossil systems. However, the look-back time that allows large BGGs to form

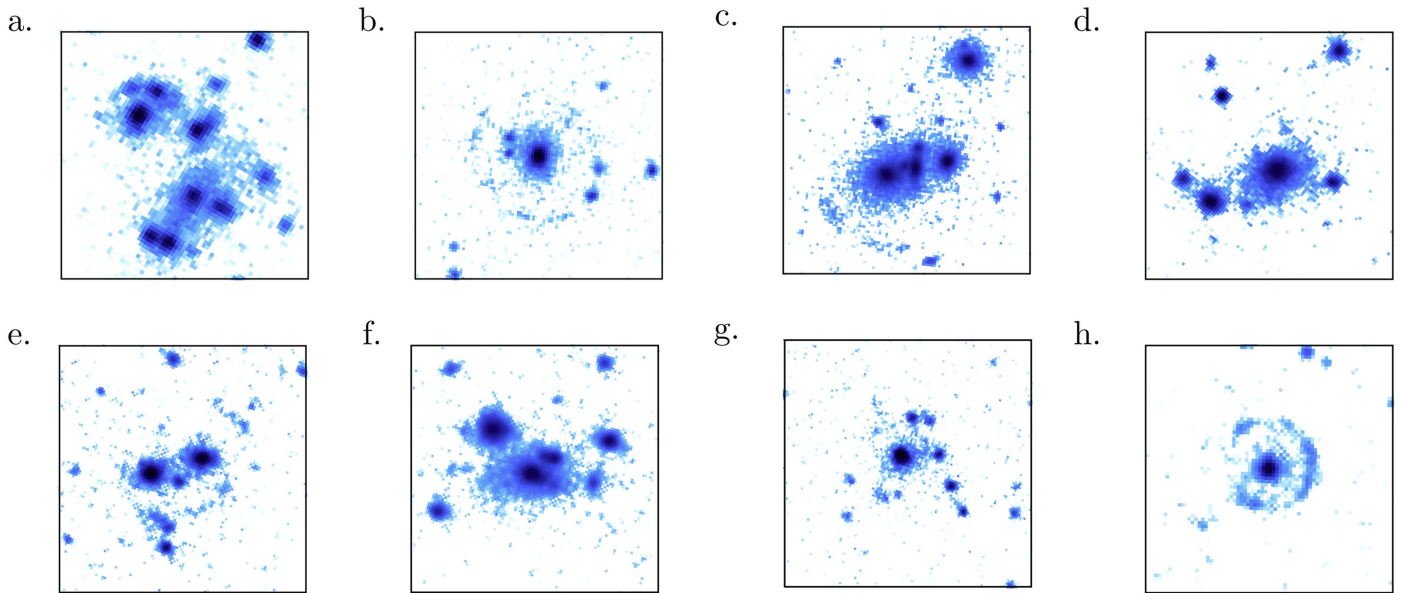


Figure 7. SDSS collage of CASSOWARY systems at various stages in BGG formation, in time order from (a) to (h). Appearing in order from upper left to bottom right along with time until fossil formation is complete: normal group (a) CSWA 23, (b) CSWA 10 (3.9 Gyr), (c) CSWA 26 (2.4 Gyr), (d) CSWA 30 (2.0 Gyr), (e) CSWA 2 (0.9 Gyr), (f) CSWA 11 (double nuclei; < 100 Myr), (g) CSWA 4 (young fossil with ongoing mergers), (h) CSWA 1 (relaxed fossil).

also allows new galaxies to fall within $0.5R_{200}$, potentially destroying a system’s fossil status before $z = 0$. To account for this chance as conservatively as possible, we define a “danger zone” for each system; this zone is the maximum projected distance from which a galaxy could free-fall inside $0.5R_{200}$ within the look-back time. The free-fall time is given by

$$t_{ff} = \frac{\pi}{2} \frac{r^{\frac{3}{2}}}{\sqrt{2G(M+m)}}, \quad (4)$$

where we took r to be the distance from the galaxy down to $0.5R_{200}$ for the group, as this is the threshold for a member to be considered in a system’s fossil classification. In an accelerating universe, the ultimate mass of a galaxy cluster in the far future is around two times the virial mass (M_{200}) at $z = 0$ (Busha et al. 2005). Since the density inside the virial radius is constant by definition, the virial radius will scale as $M_{200}^{1/3}$, making the final radius ~ 1.25 times the current R_{200} . The turnaround radius (the point beyond which matter near an overdensity of a certain mass will not collapse inward but expand) is defined as $2R_{200}$, implying that the final turnaround radius will be $\sim 2.5R_{200}$ at $z = 0$. However, since our targets are at $z > 0$, their masses have grown between when we have observed then and now. Assuming a mass growth of a factor of four between then and now, that gives a $z = 0$ virial radius of $1.6R_{200}^{obs}$ and a $z = 0$ turnaround radius of $3.2R_{200}^{obs}$. For this work, we adopt a turnaround radius of $3.0R_{200}$ and set this as the upper limit to our “danger zone.” All bright galaxies within the “danger zone” that passed our group inclusion criteria and were bright enough to violate either the Jones ($\Delta m_{12} \geq 2.0$) or Dariush ($\Delta m_{14} \geq 2.5$) fossil criteria were flagged. Groups with flagged galaxies within their “danger zone” may still be fossil progenitors; however, one cannot rule out the possibility that one or more of the flagged galaxies will eventually fall into the group potential. We found that out of the 28 strong-lensing fossil/progenitor systems in the CASSOWARY catalog, only

two (CSWA 26 and CSWA 159) have no nearby galaxies bright enough to endanger their eventual fossil statuses, making these true fossil progenitors.¹⁵

In simulations, the entire lifetime of fossil systems can be chronicled by observing when and if bright galaxies fall into the group. Observationally, it is more difficult, as we do not know the proper motions of all galaxies around the group. Spectroscopic redshifts of galaxies in and near the group can constrain the radial velocities; however, the tangential components remain unknown. This means that we cannot know for certain which bright galaxy outside $0.5R_{200}$ will fall inward. Therefore, the result that only $\sim 7\%$ of $0.2 < z < 0.7$ fossil/progenitor systems will stay fossils until $z = 0$ is an extremely conservative estimate. Spectra of observed fossils and progenitors at higher redshifts have the potential to increase this estimate, as some bright galaxies will undoubtedly be eliminated, being identified as either foreground or background.

5. Summary

The progenitors to today’s fossil systems have been shown to exist in the universe and can be located. Kanagusuku et al. (2016) found that in the Millennium Simulation most of today’s fossils finished forming their BGGs between $0.3 < z < 0.6$, which also happens to be the optimal distance to see strong gravitational lensing. The discovery of the Cheshire Cat fossil group progenitor (CSWA 2) in the CASSOWARY catalog of strong-lensing events in SDSS prompted us to analyze the remaining 57 CASSOWARY members to see whether more progenitors could be located.

In this study of CASSOWARY strong-lensing systems, we find fossil rates of $13.5\% \pm 2.8\%$ and $17.3\% \pm 2.6\%$ for the Jones et al. (2003) and Dariush et al. (2010) criteria, respectively, which is consistent with the expected rate of

¹⁵ It is interesting to note that both CSWA 26 and CSWA 159 are classified as Dariush fossils and Jones progenitors, implying that in both cases we are witnessing the formation of extremely massive BGGs compared to their respective group richnesses.

8%–20% of all groups being fossil systems (Jones et al. 2003). This contrasts with our nonlensing control fossil rates of $2.9\% \pm 1.6\%$ and $13.6\% \pm 1.2\%$, indicating the presence of a strong-lensing bias toward classical (Jones) fossil formation. Our CASSOWARY progenitor rates of $23.1\% \pm 2.5\%$ and $28.9\% \pm 2.5\%$ (Jones and Dariush, respectively) are also elevated compared to our nonlensing progenitor rates of $17.5\% \pm 1.2\%$ and $25.2\% \pm 1.1\%$. Average galaxy luminosity functions for each class of system (normal, progenitor, and fossil systems) confirmed that fossil progenitors fall between the normal and fossil fits, indicating the formation of the L^* galaxy deficit observed in fossil systems. For the CASSOWARY sample, the progenitor luminosity function showed a slight deficit of intermediate member galaxies, supporting the hypothesis that fossil BGGs are formed via cannibalization of their L^* neighbors and that we are witnessing this process in some CASSOWARY fossil progenitors.





A control sample of nonlensing groups at similar redshifts, galaxy counts, and total stellar mass was compiled to compare against the CASSOWARY lensing systems to see how the conditions leading to a strong gravitational arc near the BGG could bias the sample. It was found that while being a strong gravitational lens slightly increases the odds of a group being a fossil progenitor, it greatly increases the odds that a group will be a Jones fossil, indicating the existence of a strong-lensing bias possibly linked to the initial formation of the lensing group. Comparing the cumulative galaxy luminosity functions of the nonlensing control sample to the CASSOWARY groups showed the nonlensing progenitor function agreeing more with the nonlensing normal groups rather than transitioning to the nonlensing fossil luminosity function. This could also be an indication of the strong-lensing bias preferentially selecting the most extreme examples of fossil formation (i.e., systems with the highest mass concentration, largest intermediate-mass galaxy deficit, largest BGGs). Additionally, we observe lensing systems possessing an average of 2σ more bright galaxies than the best fit gives for galaxies outside $0.5R_{200}$. This is not seen in the nonlensing systems, further supporting the existence of a strong-lensing bias toward classical (and possibly older) fossil-like systems.

Most fossil progenitors in this study seem to be in the process of forming a massive BGG via L^* member cannibalization, making these likely progenitors of the observed cool-core fossil population seen today. We are engaged in further work on the topic of cool-core versus non-cool-core fossil progenitors using *Chandra* imaging of the hot gas of eight fossil progenitors in the CASSOWARY catalog at a range of stages in their evolution toward fossil status, from 100 Myr to 5 Gyr until sufficient merging has concluded, to establish the required r -band magnitude gap. Our goal is to observe the evolution of the hot gas component of a fossil progenitor and whether or not a cool core is present as the BGG forms (Johnson et al. 2018, in preparation).

We thank William Keel, Jeremy Bailin, Yuanyuan Su MacLellan, Eddie Johnson, and Spring Johnson for useful

conversations and constructive feedback. We also thank an anonymous referee for numerous helpful suggestions. This work was supported by *Chandra* grant GO6-17106X and *HST* grant HST-GO-14362.003-A.

ORCID iDs

Jimmy A. Irwin  <https://orcid.org/0000-0003-4307-8521>
 Ka-Wah Wong  <https://orcid.org/0000-0002-5267-2867>
 W. Peter Maksym  <https://orcid.org/0000-0002-2203-7889>
 Eleazar R. Carrasco  <https://orcid.org/0000-0002-7272-9234>

References

- Behroozi, P. S., Conroy, C., & Wechsler, R. H. 2010, *ApJ*, **717**, 379
 Belokurov, V., Evans, N. W., Hewett, P. C., et al. 2009, *MNRAS*, **392**, 104
 Busha, M. T., Evrard, A. E., Adams, F. C., & Wechsler, R. H. 2005, *MNRAS*, **363**, L11
 Chilingarian, I. V., Melchior, A.-L., & Zolotukhin, I. Y. 2010, *MNRAS*, **405**, 1409
 Dariush, A. A., Raychaudhury, S., Ponman, T. J., et al. 2010, *MNRAS*, **405**, 1873
 Farhang, A., Khosroshahi, H. G., Mamon, G. A., Dariush, A. A., & Raouf, M. 2017, *ApJ*, **840**, 58
 Gehrels, N. 1986, *ApJ*, **303**, 336
 Gozaliasl, G., Finoguenov, A., Khosroshahi, H. G., et al. 2014, *A&A*, **566**, A140
 Grillo, C., Christensen, L., Gallazzi, A., & Rasmussen, J. 2013, *MNRAS*, **433**, 2604
 Hansen, S. M., McKay, T. A., Wechsler, R. H., et al. 2005, *ApJ*, **633**, 122
 Hickson, P. 1982, *ApJ*, **255**, 382
 Irwin, J. A., Dupke, R., Carrasco, E. R., et al. 2015, *ApJ*, **806**, 268
 Jones, L. R., Ponman, T. J., Horton, A., et al. 2003, *MNRAS*, **343**, 627
 Kanagasku, M. J., Díaz-Giménez, E., & Zandivarez, A. 2016, *A&A*, **586**, A40
 Khosroshahi, H. G., Jones, L. R., & Ponman, T. J. 2004, *MNRAS*, **349**, 1240
 Khosroshahi, H. G., Maughan, B. J., Ponman, T. J., & Jones, L. R. 2006, *MNRAS*, **369**, 1211
 Khosroshahi, H. G., Ponman, T. J., & Jones, L. R. 2007, *MNRAS*, **377**, 595
 Kitzbichler, M. G., & White, S. D. M. 2008, *MNRAS*, **391**, 1489
 La Barbera, F., de Carvalho, R. R., de La Rosa, I. G., et al. 2010, in *ASP Conf. Ser. Galaxies in Isolation: Exploring Nature Versus Nurture*, ed. L. Verdes-Montenegro (San Francisco, CA: ASP), 225
 Lieder, S., Mieske, S., Sánchez-Janssen, R., et al. 2013, *A&A*, **559**, A76
 Lopes, P. A. A., de Carvalho, R. R., Kohl-Moreira, J. L., & Jones, C. 2009, *MNRAS*, **399**, 2201
 Oguri, M. 2014, *MNRAS*, **444**, 147
 Ponman, T. J., Allan, D. J., Jones, L. R., et al. 1994, *Natur*, **369**, 462
 Raouf, M., Khosroshahi, H. G., Ponman, T. J., et al. 2014, *MNRAS*, **442**, 1578
 Roche, N., Bernardi, M., & Hyde, J. 2009, *MNRAS*, **398**, 1549
 Rykoff, E. S., Koester, B. P., Rozo, E., et al. 2012, *ApJ*, **746**, 178
 Stark, D. P., Auger, M., Belokurov, V., et al. 2013, *MNRAS*, **436**, 1040
 Sun, M., Forman, W., Vikhlinin, A., et al. 2004, *ApJ*, **612**, 805
 Sun, M., Voit, G. M., Donahue, M., et al. 2009, *ApJ*, **693**, 1142
 Trentham, N. 1995, *MNRAS*, **277**, 616
 Trevisan, M., Mamon, G. A., & Khosroshahi, H. G. 2017, *MNRAS*, **464**, 4593
 von Benda-Beckmann, A. M., D’Onghia, E., Gottlöber, S., et al. 2008, *MNRAS*, **386**, 2345
 Wechsler, R. H., Bullock, J. S., Primack, J. R., Kravtsov, A. V., & Dekel, A. 2002, *ApJ*, **568**, 52
 Wen, Z. L., Han, J. L., & Liu, F. S. 2012, *ApJS*, **199**, 34
 Westra, E., Geller, M. J., Kurtz, M. J., Fabricant, D. G., & Dell’Antonio, I. 2010, *PASP*, **122**, 1258
 Wiesner, M. P., Lin, H., Allam, S. S., et al. 2012, *ApJ*, **761**, 1
 Zarattini, S., Aguerri, J. A. L., Sánchez-Janssen, R., et al. 2015, *A&A*, **581**, A16